

Electronic Supplementary Information

Bronze, silver and gold: functionalized group 11 organotin sulfide clusters

Jens P. Eußner and Stefanie Dehnen*

Philipps-Universität Marburg, Fachbereich Chemie and Wissenschaftliches Zentrum für Materialwissenschaften (WZMW), Hans-Meerwein-Straße, D-35043 Marburg, Germany. E-mail: dehnen@chemie-uni-marburg.de; Fax: +49 6421 2825653; Tel: +49 6421 2825751.

1. Synthesis details

General: All manipulations were performed under argon atmosphere. All solvents were dried and freshly distilled prior to use. $[(R^1Sn)_3S_4Cl]$,¹ $(Me_3Si)_2S$,² $[Cu(PPh_3)_3Cl]$ ³ and $[Ag(PPh_3)_3Cl]$ ⁴ were prepared according to reported methods. $N_2H_4 \cdot H_2O$ and $[Au(PPh_3)Cl]$ were purchased from Aldrich.

1H NMR, ^{13}C NMR, ^{31}P NMR and ^{119}Sn NMR measurements were carried out using a Bruker DRX 250 MHz, DRX 300 MHz, DRX 400 MHz and DRX 500 MHz spectrometer at 25°C. The chemical shifts were quoted in ppm relative to the residual protons of deuterated solvents in 1H NMR and ^{13}C NMR. 85% H_3PO_4 was used as internal standard for ^{31}P NMR measurements. Me_4Sn was used as internal standard for ^{119}Sn NMR measurements. Owing to bad solubility and thus low concentration of **1–4** in all common solvents, it was not possible to receive any ^{119}Sn NMR signals. Elemental analysis was performed on an Elementar vario micro apparatus. Energy-dispersive X-ray spectroscopy analysis, EDX, was performed using the EDX device Voyager 4.0 of Noran Instruments coupled with the electron microscope CamScan CS 4DV. Data acquisition was performed with an acceleration voltage of 20 kV and 100 s accumulation time. All complexes decomposed at about 150 °C.

Synthesis of 1: $[(R^1Sn)_3S_4Cl]$ (0.100 g, 0.122 mmol) and $[Cu(PPh_3)_3Cl]$ (0.186 g, 0.210 mmol) were dissolved in CH_2Cl_2 (5 mL). $(Me_3Si)_2S$ (0.069 g, 0.386 mmol) was added at room temperature and the solution was stirred for 12 h. The resulting yellow solution was layered with *n*-hexane (5 mL). Pale yellow crystals formed within one day. The crystals were collected and dried in high vacuum. Yield: 8 mg (3.8 mmol, 6% calculated on the basis of $[(R^1Sn)_3S_4Cl]$); 1H -NMR (300 MHz, CD_2Cl_2 , 25 °C): δ = 1.34 (s, $^3J_{1H-119Sn}$ = 158 Hz, CMe_2 24H), 2.27 (s, Me, 12H), 2.90 (s, $^3J_{1H-119Sn}$ = 159 Hz, CH_2 , 8H), 7.2–7.4 (m, Ph, 36H) ppm; $^{31}P\{^1H\}$ -NMR (101 MHz, $CDCl_3$, 25 °C): 29.8 ppm; EDX: Cu/P/S/Sn calcd: 0.25:0.25:1.00:0.75; found 0.26:0.27:1.00:0.74 (Cl was not considered because of CH_2Cl_2 solvent molecules).

Synthesis of 2: $[(R^1Sn)_3S_4Cl]$ (0.100 g, 0.122 mmol) and $[Cu(PPh_3)_3Cl]$ (0.108 g, 0.122 mmol) were dissolved in CH_2Cl_2 (10 mL). $(Me_3Si)_2S$ (0.066 g, 0.366 mmol) was added at room temperature and the solution was stirred for 12 h. The resulting yellow solution was layered with *n*-hexane (10 mL). Pale yellow crystals formed within one day. The crystals were collected and dried in high vacuum. Yield: 4 mg (0.0013 mmol, 4% calculated on the basis of $[(R^1Sn)_3S_4Cl]$); $^{31}P\{^1H\}$ -NMR (101 MHz, $CDCl_3$, 25 °C): 29.8 ppm; EDX: Cl/Cu/P/S/Sn calcd: 0.14:0.14:0.14:1.00:0.71; found 0.19:0.10:0.14:1.00:0.67.

Synthesis of 3: [(R¹Sn)₃S₄Cl] (0.100 g, 0.122 mmol) and [Ag(PPh₃)₃Cl] (0.341 g, 0.367 mmol) were dissolved in CH₂Cl₂ (7 mL). (Me₃Si)₂S (0.109 g, 0.610 mmol) was added at –78 °C. The solution was carefully warmed up to room temperature in a time of 24 h. The resulting colorless precipitate was filtered off and resolved in CH₂Cl₂ (14 mL). The solution was layered with *n*-hexane (14 mL). Pale yellow crystals formed within 2 weeks. The crystals were collected and dried in high vacuum. Yield: 2 mg (0.006 mmol, 2% calculated on the basis of [(R¹Sn)₃S₄Cl]); EDX: Ag/Cl/P/S/Sn calcd: 0.14:0.14:1.00:0.71; found 0.14:0.13:0.14:1.00:0.69.

Synthesis of 4: [(R¹Sn)₃S₄Cl] (0.100 g, 0.122 mmol) and [Ag(PPh₃)₃Cl] (0.341 g, 0.367 mmol) were dissolved in CH₂Cl₂ (7 mL). (Me₃Si)₂S (0.109 g, 0.610 mmol) was added at –78 °C. The solution was carefully warmed up to room temperature in a time of 24 h. The resulting colourless precipitate was filtered off and resolved in CH₂Cl₂ (14 mL). N₂H₄·H₂O (0.03 mL) was added to the deep red solution. It was stirred for 30 min at room temperature. The solution was layered with *n*-hexane (14 mL). Orange crystals formed within one day. The crystals were collected and dried in high vacuum. Yield: 32 mg (0.0074 mmol, 20% calculated on the basis of [(R¹Sn)₃S₄Cl]); EDX: Ag/S/Sn calcd: 0.50:1.00:0.50; found 0.48:1.00:0.48.

Synthesis of 5: [(R¹Sn)₃S₄Cl] (0.100 g, 0.122 mmol) and [Au(PPh₃)Cl] (0.182 g, 0.367 mmol) were dissolved in CH₂Cl₂ (7 mL). (Me₃Si)₂S (0.087 g, 0.488 mmol) was added at room temperature and the solution was stirred for 24 h. The resulting colourless solution was layered with *n*-hexane (7 mL). Colourless crystals formed within one day. The crystals were collected and dried in high vacuum. Yield: 115 mg (0.077 mmol, 44% calculated on the basis of [(R¹Sn)₃S₄Cl]); elemental analysis (%): calc. for C₄₈H₅₂Au₂O₂P₂S₄Sn₂: C 38.89, H 3.54, N 0, S 8.65, found C 37.93, H 3.55, N 0, S 8.64; ¹H-NMR (300 MHz, CD₂Cl₂, 25 °C): δ = 1.20 (s, ³J_{1H-119Sn} = 125 Hz, CMe₂ 12H), 2.01 (s, Me, 6H), 2.65 (s, ³J_{1H-119Sn} = 135 Hz, CH₂, 4H), 7.28–7.65 (m, Ph, 36H) ppm; ¹³C-NMR (75 MHz, CD₂Cl₂, 25 °C): δ = 26.44 (Me₂), 30.62 (Me), 36.90 (SnC), 56.30 (CH₂), 129.47 (Ph), 129.62 (Ph), 131.19 (Ph), 131.89 (Ph), 134.85 (Ph), 135.04 (Ph), 211.53 (CO) ppm; ³¹P{¹H}-NMR (101 MHz, CDCl₃, 25 °C): 38.1 ppm; ¹¹⁹Sn-NMR (149 MHz, CD₂Cl₂, 25 °C): δ = 51.2 ppm; EDX: Au/P/S/Sn calcd: 0.50:1.00:0.50:0.50; found 0.47:0.55:1.00:0.50.

Synthesis of 6: [(R¹Sn)₃S₄Cl] (0.100 g, 0.122 mmol) and [Au(PPh₃)Cl] (0.182 g, 0.367 mmol) were dissolved in CH₂Cl₂ (7 mL). (Me₃Si)₂S (0.087 g, 0.488 mmol) was added at room temperature and the solution was stirred for 24 h. N₂H₄·H₂O (0.03 mL) was added to the solution. It was stirred for 30 min at room temperature. The resulting white precipitate was removed by filtration. The colourless solution was layered with *n*-hexane (7 mL). Colourless crystals formed

within one day. The crystals were collected and dried in high vacuum. Yield: 110 mg (0.07 mmol, 38% calculated on the basis of $[(R^1Sn)_3S_4Cl]$); elemental analysis (%): calc. for $C_{48}H_{56}Au_2N_4P_2S_4Sn_2 \cdot 2CH_2Cl_2$: C 35.74, H 3.60, N 3.33, S 7.63, found C 36.60, H 3.72, N 3.46, S 7.45; 1H -NMR (300 MHz, CD_2Cl_2 , 25 °C): δ = 1.22 (s, CMe_2 12H), 1.61 (s, Me, 6H), 2.32 (s, CH_2 , 4H), 4.87 (br s, NH_2 , 4H), 7.17–7.38 (m, Ph, 36H) ppm; $^{31}P\{^1H\}$ -NMR (101 MHz, CD_2Cl_2 , 25 °C): 39.0 ppm; ^{119}Sn -NMR (149 MHz, CD_2Cl_2 , 25 °C): δ = -56.7 ppm; EDX: Au/P/S/Sn calcd: 0.50:1.00:0.50:0.50; found 0.46:0.55:1.00:0.50.

Further observations: Compounds **1–3** can be viewed as intermediates at the reaction towards larger clusters. In general, it should be possible to substitute the remaining Cl substituents by S atoms. However, although excess of $(Me_3Si)_2S$ was present in the synthesis of **1–3**, no such substitution occurred under the chosen reactions conditions and within the time scale explored. Reflux of the reaction mixtures for 24 h, or stirring for one week at room temperature lead to the formation of deep red solutions in any case. However, no single-crystals could be isolated from these solutions, neither upon layering with different solvents, or slow evaporation, or cooling to low temperatures. Instead, slow decomposition took place under formation of dark precipitate. ^{31}P NMR spectroscopy reveals that PPh_3 is present in these solutions as a sign of decomposition by split-off of the phosphine ligands. After two weeks at room temperature, we observed $S=PPh_3$ by ^{31}P NMR spectroscopy with very low intensity besides PPh_3 , indicating ongoing decomposition of the M/Sn/S cluster core. Finally, it is not clear what inhibits the formation and isolation of larger aggregates. Most likely, the metastable character of the clusters is increased when growing, thus decomposition reactions win the thermodynamic competition. Oxidation of PPh_3 was ruled out via ^{31}P NMR spectroscopy. A possible oxidation of Cu^I was probed by addition of an aqueous NH_3 solution to the mother liquor of the crystals. A phase boundary formed, but no color change was observed; in contrast, a crosscheck using a highly diluted Cu^{2+} solution ($1 \mu mol \cdot L^{-1}$) in CH_2Cl_2 was positive in that a blue color appeared immediately at the phase boundary.

In the presented work, structures and compositions of the ternary complexes vary. All ternary complexes were generated by re-arrangement of the inorganic core within solution, which comes along with a loss of either M, Sn and/or S atoms from the clusters owing to different stoichiometry. The isolation of the complexes was achieved by systematic variation of the stoichiometry of the reactants and is finally due to their low solubility in the chosen solvents; this allowed for rapid crystallization – prior to complete decomposition of the hybrid compounds into the thermodynamically stable, binary Sn/S or M/S (M = Cu, Ag, Au) phases, that only occurred

as side products here. All given yields are those for isolated single-crystals. In the case of M = Ag, a dark precipitate of AgS occurs within one day. In the case of M = Au, the main side product is $[(R^1Sn)_4S_6]$, which remains in solution as confirmed by NMR spectroscopy. For these reasons, the yields of the presented reactions are moderate to low, especially for compounds **1–3**.

2. Details of the X-ray diffraction measurements, structure solutions and refinements

General

Data of the X-ray structure analysis: T = 100 K, graphite monochromator, imaging plate detector Stoe IPDS2/2T. All structures were solved by direct methods in SHELXS97 refined by full-matrix-least-squares refinement against F^2 in SHELXL97 (Sheldrick, 1997).⁵ Where possible, H atoms were inserted assuming idealized geometry and refined riding on their parent atoms (with $U_{eq} = nU_{eq}$ (parent atom), where $n = 1.2$ for H atoms in methylene groups and $n = 1.5$ for H atoms in methyl groups. Crystallographic refinement details are provided in Tables S1 (**1–4**) and S2 (**5, 6, (Me₃Si)₂S**).

Table S1. Crystallographic and refinement details of **1–4** at 100 K (Mo K_{α} radiation, $\lambda = 0.71073$ Å).

Compound	1 ·4CH ₂ Cl ₂	2	3 ·[(R ¹ Sn) ₄ S ₆]	4 ·3.5CH ₂ Cl ₂
empirical formula	C ₆₄ H ₈₂ Cl ₁₀ Cu ₂ O ₄ P ₂ S ₈ Sn ₆	C ₈₄ H ₁₁₈ Cl ₂ Cu ₂ O ₈ P ₂ S ₁₄ Sn ₁₀	C ₈₄ H ₁₁₈ Ag ₂ Cl ₂ O ₈ P ₂ S ₁₄ Sn ₁₀	C _{63.5} H ₁₂₇ Ag ₁₀ Cl ₇ N ₂₀ S ₂₀ Sn ₁₀
fw /g·mol ⁻¹	2427.44	3151.44	3240.10	4325.80
crystal color and shape	yellow block	yellow plate	yellow block	orange octahedron
crystal size /mm ³	0.20x0.17x0.17	0.15x0.12x0.07	0.20x0.20x0.18	0.17x0.14x0.14
crystal system	triclinic	triclinic	triclinic	tetragonal
space group	<i>P</i> -1	<i>P</i> -1	<i>P</i> -1	<i>I</i> 4 ₁ / <i>a</i>
<i>a</i> /Å	12.6985(5)	12.4911(10)	12.5280(4)	30.8293(3)
<i>b</i> /Å	13.1259(5)	15.0900(13)	15.2617(5)	30.8293(3)
<i>c</i> /Å	15.4384(8)	15.4207(11)	15.4195(5)	54.2835(7)
α /deg	115.138(3)	91.029(6)	91.365(3)	90
β /deg	101.519(4)	102.416(6)	102.845(2)	90
γ /deg	101.370(3)	101.294(6)	100.328(2)	90
<i>V</i> /Å ³	2164.22(16)	2778.2(4)	2821.60(16)	51593.5(10)
<i>Z</i>	1	1	1	16
ρ_{calcd} /g·cm ⁻³	1.862	1.884	1.907	2.228
$\mu(\text{Mo } K_{\alpha})$ /mm ⁻¹	2.763	2.965	2.890	3.885
absorption correction type	numerical	numerical	sphere	gaussian
min./max. transmission	0.498/0.706	0.685/0.811	0.419/0.429	0.317/0.332
2θ range /deg	3.04/54.50	2.70/50.00	2.70/54.24	3.00/52.00
no. of meas. reflns.	19199	19994	28531	135399
<i>R</i> (int)	0.0627	0.0961	0.1340	0.1191
indep. reflns.	9141	9740	11905	25331
indep. reflns. (<i>I</i> > 2 σ (<i>I</i>))	7723	4688	10828	19628
no. of parameters	439	562	562	1234
<i>R</i> ₁ (<i>I</i> > 2 σ (<i>I</i>))/ <i>wR</i> ₂ (all data)	0.0288/0.0714	0.0460/0.1033	0.0374/0.0701	0.0406/0.0975
<i>S</i> (all data)	0.961	0.698	1.060	1.009
max. peak/hole/ e ⁻ ·Å ⁻³	1.04/-1.26	1.78/-0.69	2.06/-1.62	2.78/-1.63

Table S2. Crystallographic and refinement details of **5**, **6** and (Me₃Si)₂S at 100 K (Mo K_α radiation, $\lambda = 0.71073 \text{ \AA}$).

Compound	5	6 ·5CH ₂ Cl ₂	(Me ₃ Si) ₂ S
empirical formula	C ₄₈ H ₅₂ Au ₂ O ₂ P ₂ S ₄ Sn ₂	C ₅₃ H ₆₆ Au ₂ Cl ₁₀ N ₄ P ₂ S ₄ Sn ₂	C ₆ H ₁₈ SSi ₂
fw /g·mol ⁻¹	1482.39	1935.09	178.44
crystal color and shape	colourless plate	colourless plate	colourless block
crystal size /mm ³	0.30x0.12x0.10	0.37x0.21x0.01	0.80x0.30x0.30
crystal system	monoclinic	triclinic	monoclinic
space group	<i>P</i> 2 ₁ / <i>c</i>	<i>P</i> -1	<i>C</i> 2/ <i>c</i>
<i>a</i> / \AA	14.5079(6)	8.5220(5)	18.407(4)
<i>b</i> / \AA	12.1592(5)	12.3547(9)	5.7619(7)
<i>c</i> / \AA	15.0025(6)	17.3906(10)	11.610(2)
α /deg	90	77.566(5)	90
β /deg	103.390(3)	83.985(5)	113.848(15)
γ /deg	90	71.477(5)	90
<i>V</i> / \AA^3	2574.57(18)	1694.12(19)	1126.2(4)
<i>Z</i>	2	1	4
ρ_{calcd} /g·cm ⁻³	1.912	1.90	0.438
$\mu(\text{Mo K}\alpha)$ /mm ⁻¹	6.900	5.648	0.438
absorption correction type	numerical	multi-scan	numerical
min./max. transmission	0.264/0.601	0.010/0.470	0.696/0.832
2θ range /deg	4.42/53.44	2.54/53.64	4.84/50.20
no. of meas. reflns.	16529	15920	976
<i>R</i> (int)	0.0751	0.0753	0.0972
indep. reflns.	5448	7154	976
indep. reflns. ($I > 2\sigma(I)$)	3561	6449	755
no. of parameters	274	370	46
<i>R</i> ₁ ($I > 2\sigma(I)$)/ <i>wR</i> ₂ (all data)	0.0453/0.1086	0.0756/0.1986	0.0942/0.2393
<i>S</i> (all data)	0.889	1.205	1.202
max. peak/hole/ e ⁻ · \AA^{-3}	1.97/-1.43	2.85/-2.43	0.87/-0.32

Compound 1: The compound crystallizes with four molecules dichloromethane per formula unit in the triclinic space group $P\bar{1}$ with $Z = 1$. The highest peak of $1.04 \text{ e}/\text{\AA}^3$ on the difference Fourier map was observed 1.04 \AA apart from Sn2. Selected intermolecular parameters are outlined in Table S3.

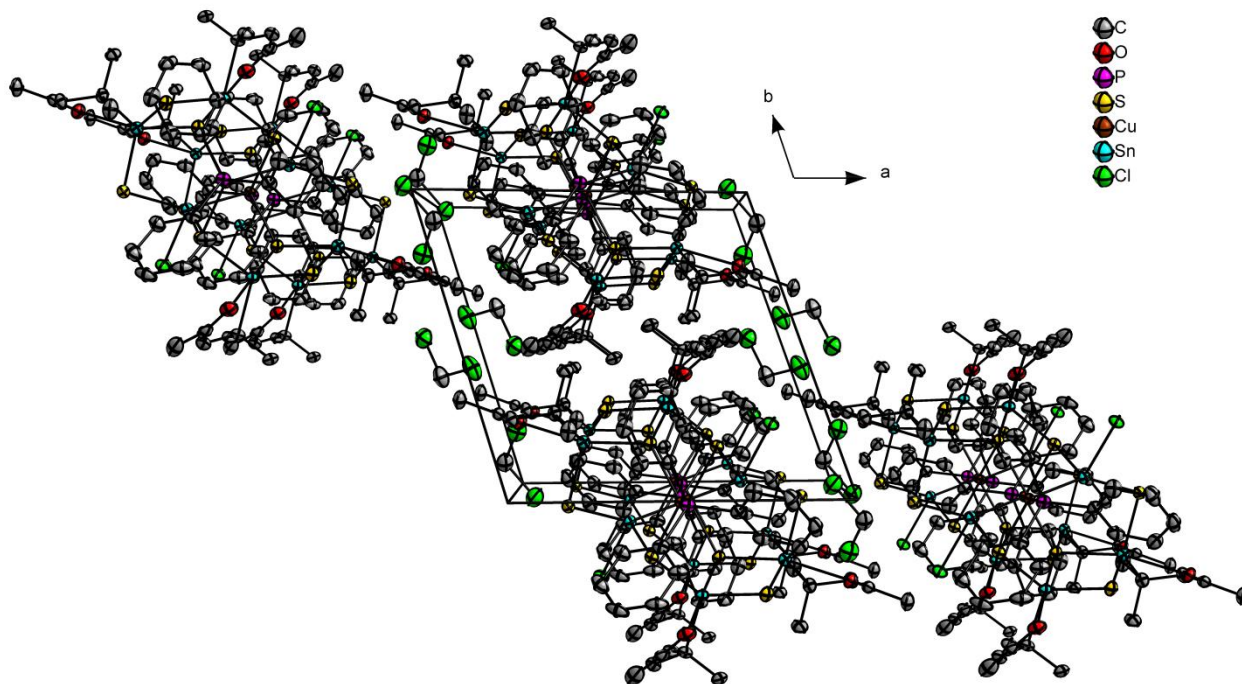


Figure S1. View along [001] in $1 \cdot 4\text{CH}_2\text{Cl}_2$. H atoms are omitted for clarity.

Thermal ellipsoids are drawn at 50% probability.

Compound 2: The compound crystallizes with $[(R^I Sn)_4 S_6]$ ($R^I = CMe_2CH_2C(O)Me$) per formula unit in the triclinic space group $P\bar{1}$ with $Z = 1$. The highest peak of $1.78 \text{ e}/\text{\AA}^3$ on the difference Fourier map was observed 1.05 \AA apart from Sn2. Selected intermolecular parameters are outlined in Table S3.

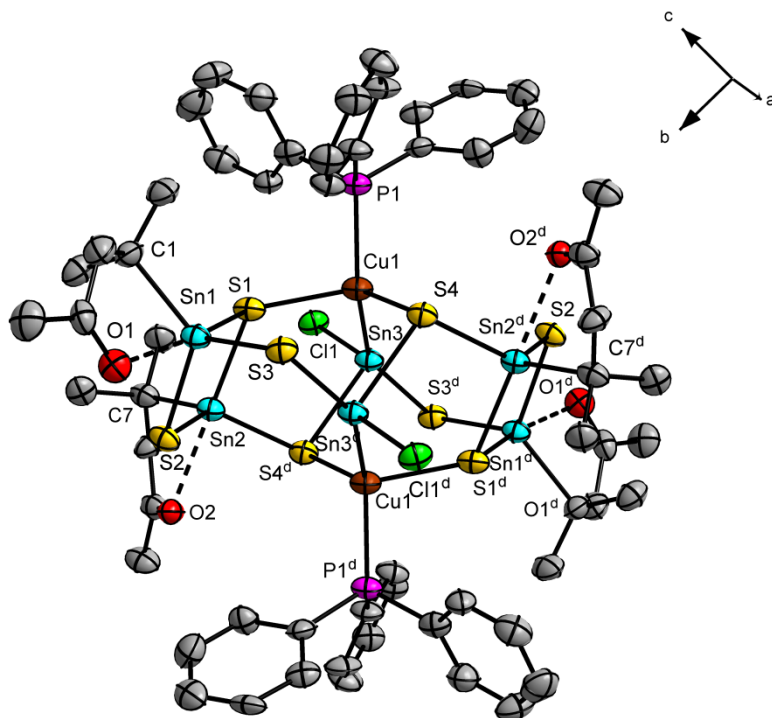


Figure S2. Molecular structure of $[(R^I Sn^{IV})_4(Sn^{II}Cl)_2(CuPPh_3)_2S_8]$ in **2**. H atoms are omitted for clarity. Thermal ellipsoids are drawn at 50% probability. $d = -x, 2-y, -z$.

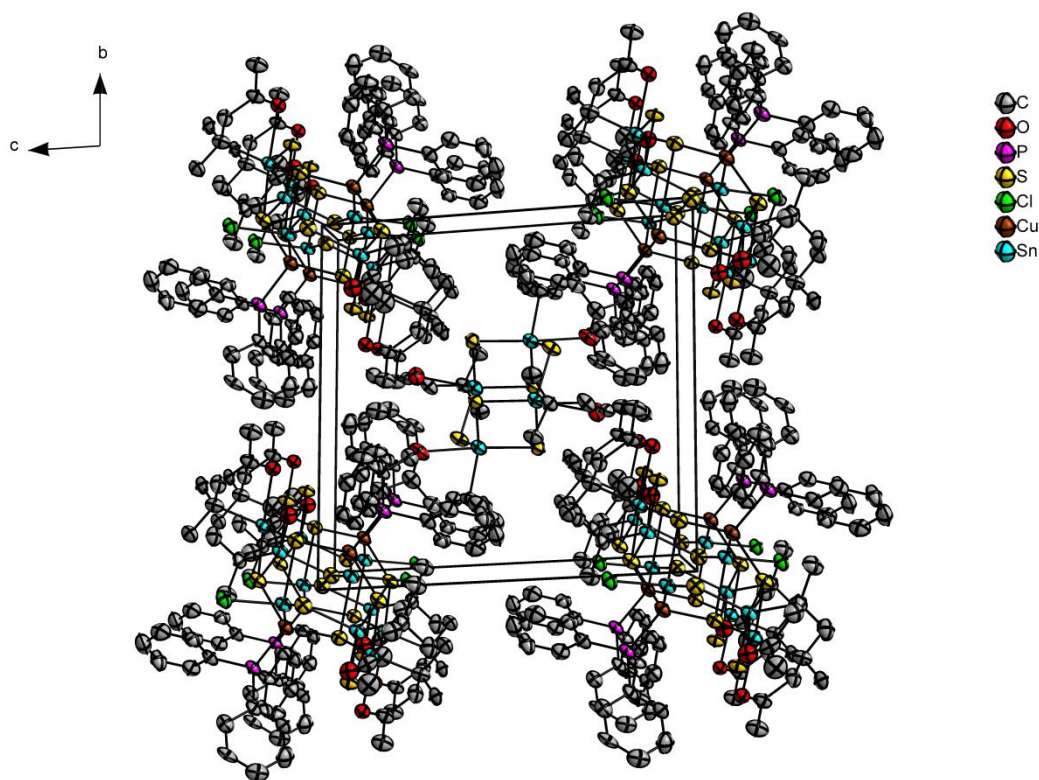


Figure S3. View along [100] in $2 \cdot [(R^I \text{Sn})_4 \text{S}_6]$. H atoms are omitted for clarity. Thermal ellipsoids are drawn at 50% probability.

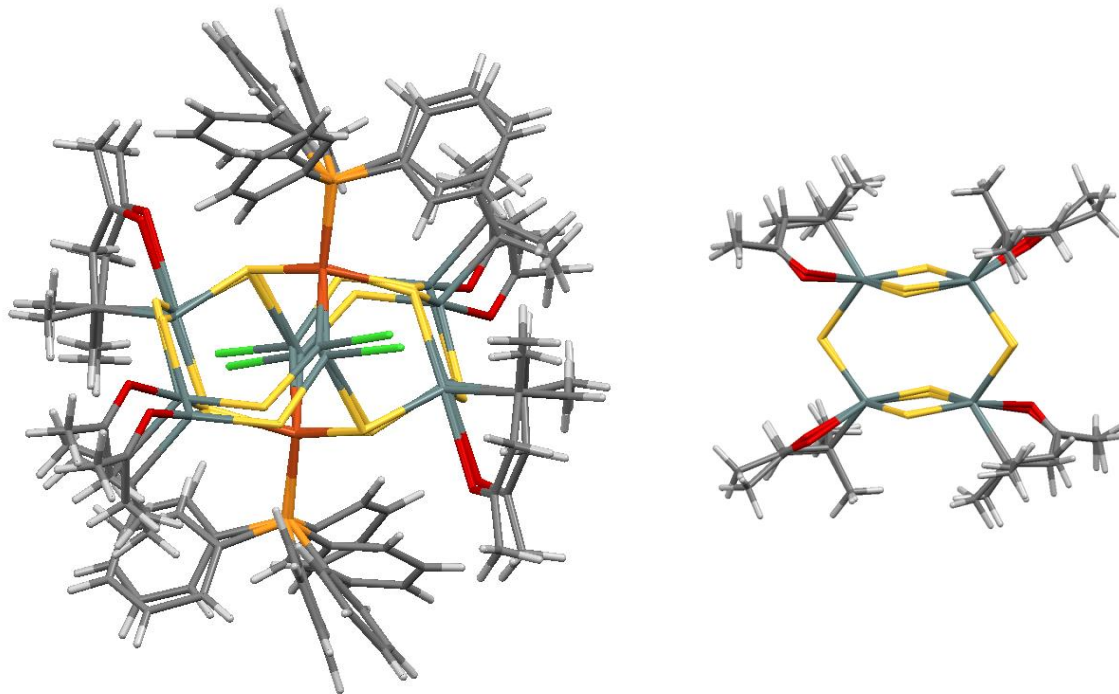


Figure S4. Superposition of the $[(R^I \text{Sn}^{IV})_4(\text{Sn}^{II}\text{Cl})_2(\text{CuPPh}_3)_2\text{S}_8]$ units in $1 \cdot 4\text{CH}_2\text{Cl}_2$ and 2 (left) and of the $[(R^I \text{Sn})_4 \text{S}_6]$ complexes in $2 \cdot [(R^I \text{Sn})_4 \text{S}_6]$ and $[(R^I \text{Sn})_4 \text{S}_6]$ (from SURQEC), respectively (right).

Compound 3: The compound crystallizes with $[(R^1Sn)_4S_6]$ ($R^1 = CMe_2CH_2C(O)Me$) per formula unit in the triclinic space group $P\bar{1}$ with $Z = 1$. The crystal structure is isostructural to **2**. The highest peak of $2.07 e/\text{\AA}^3$ on the difference Fourier map was observed 0.86\AA apart from Sn2. Selected intermolecular parameters are outlined in Table S3.

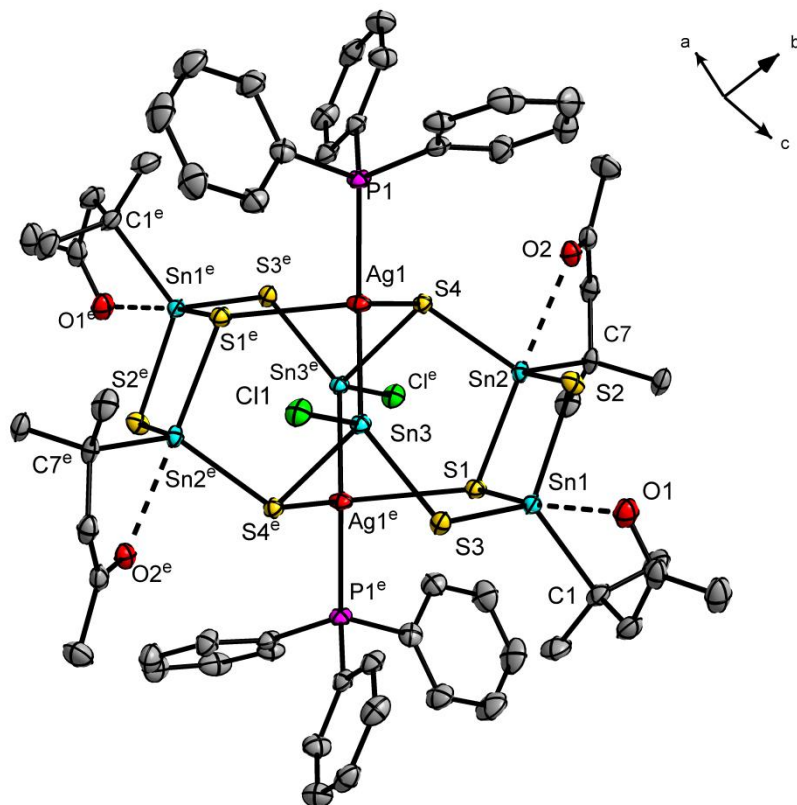


Figure S5. Molecular structure of **3**. H atoms are omitted for clarity.

Thermal ellipsoids are drawn at 50% probability. e = $-x, -y, -z$.

Table S3. Selected structural parameters [\AA , $^\circ$] of **1**·4CH₂Cl₂, **2** and **3**·[(R¹Sn)₄S₆].

compound	1 ·4CH ₂ Cl ₂	2	3
Sn1–C1	2.183(3)	2.209(11)	2.196(3)
Sn1–O1	2.516(2)	2.469(7)	2.493(2)
Sn1–S1	2.5058(8)	2.519(3)	2.4910(7)
Sn1–S2	2.4227(8)	2.422(3)	2.4221(7)
Sn1–S3	2.3654(8)	2.377(3)	2.3883(7)
Sn1–C7	2.192(3)	2.182(11)	2.179(3)
Sn1–O2	2.537(2)	2.512(7)	2.5301(19)
Sn2–S1	2.4692(7)	2.481(3)	2.4603(6)
Sn2–S2	2.4140(8)	2.419(3)	2.4194(7)
Sn2–S4 ^{a,d,e}	2.4142(8)	2.420(3)	2.4192(6)
Sn3–Cl1	2.4713(8)	2.479(3)	2.4607(7)
Sn3–S3 ^{a,d,e}	2.4983(9)	2.508(3)	2.4841(7)
Sn3–S4 ^{a,d,e}	2.5467(8)	2.557(3)	2.5337(6)
Sn3–Cu/Ag1	2.6054(4)	2.5982(15)	2.6803(3)
Cu/Ag1–P1	2.2590(8)	2.267(3)	2.4514(7)
Cu/Ag1–S1	2.3626(9)	2.376(3)	2.6783(7)
Cu/Ag1–S4	2.3166(8)	2.337(3)	2.5532(7)
O1–Sn1–S1	164.69(6)	165.48(18)	162.64(5)
O2–Sn2–S1	177.13(6)	173.81(19)	173.07(5)
S1–Sn1–S2	91.24(3)	91.41(9)	91.39(2)
S1–Sn2–S2	92.34(3)	92.37(10)	92.20(2)
Cu/Ag1–Sn3–S3 ^{a,d,e}	149.75(2)	150.38(8)	143.867(17)
Cu/Ag1–Sn3–S4 ^{a,d,e}	107.60(2)	105.73(7)	109.025(17)
Cl1–Sn3–Cu/Ag1	111.23(2)	111.80(7)	111.720(18)
Cl1–Sn3–S3 ^{a,d,e}	90.20(3)	88.77(9)	92.41(2)
Cl1–Sn3–S4 ^{a,d,e}	95.70(3)	97.45(9)	97.07(2)
S3–Sn3 ^{a,d,e} –S4	90.44(3)	91.73(9)	93.42(2)
Sn1–S1–Sn2	86.57(2)	86.25(9)	86.92(2)
Sn1–S2–Sn2	89.70(3)	89.83(9)	89.41(2)
Sn1–S1–Cu/Ag1	120.99(3)	120.48(12)	117.63(3)
Sn2–S1–Cu/Ag1	120.14(3)	119.13(12)	116.39(2)
Sn1–S3–Sn3 ^{a,d,e}	95.46(3)	96.59(10)	97.63(3)
Sn2–S4 ^{a,d,e} –Sn3	100.49(3)	102.70(10)	104.93(2)
Sn2–S4 ^{a,d,e} –Cu/Ag1	106.52(3)	107.07(11)	100.24(3)
Sn3–Cu/Ag1–P1	115.40(3)	125.59(9)	131.23(2)
S1–Cu/Ag1–S4	116.75(3)	118.47(11)	114.81(2)

symmetry code: a = 1–x, –y, –z (**1**·4CH₂Cl₂); d = –x, 2–y, –z (**2**); –x, –y, –z (**3**·[(R¹Sn)₄S₆]).

Compound 4: The compound crystallizes with 3.5 molecules of dichloromethane per formula unit in the tetragonal space group $I 4_1/a$ with $Z = 16$. N–H hydrogen atoms were not found on the difference Fourier map. One organic substituent was found to be disordered. The disorder was modeled in two positions for the atom pairs C32A/C32B, C33A/C33B, C34A/C34B, N12A/N12B (occupancy 0.580(13)/ 0.420(13)). Additionally, two dichloromethane molecules are disordered. In the first molecule C62, Cl3, Cl4A/Cl4B the position of Cl4 was split in two positions (occupancy 0.607(10)/0.393(10)). In the second molecule C64A/C64B, Cl7, Cl8 the position of C64 was split in two positions (occupancy 0.5/0.5). The molecular geometry and thermal displacement parameters of the disordered solvent molecules were restrained and partially refined isotropically. The dichloromethane molecule C63, Cl5, Cl6 is disordered by symmetry and therefore exhibits occupancy of 0.5. The highest peak of $2.77 \text{ e}/\text{\AA}^3$ on the difference Fourier map was observed 2.19 \AA apart from N12A. Selected intermolecular parameters are outlined in Table S4.

Table S4. Selected structural parameters [\AA , $^\circ$] of $4 \cdot 3.5\text{CH}_2\text{Cl}_2$.

C1–Sn1	2.186(6)	N19–Sn10	2.443(5)
C7–Sn2	2.174(7)	S1–Sn1	2.4189(17)
C13–Sn3	2.181(6)	S1–Ag3	2.4543(16)
C19–Sn4	2.170(6)	S1–Sn2	2.5827(15)
C25–Sn5	2.175(7)	S2–Sn1	2.3865(16)
C31–Sn6	2.187(7)	S2–Ag1	2.4340(16)
C37–Sn7	2.177(7)	S2–Ag2	2.5199(18)
C43–Sn8	2.185(6)	S3–Sn2	2.4045(17)
C49–Sn9	2.170(6)	S3–Sn1	2.5536(15)
C55–Sn10	2.184(6)	S4–Sn4	2.5160(16)
N1–Sn1	2.478(5)	S4–Sn3	2.5222(16)
N3–Sn2	2.382(5)	S4–Ag3	2.6752(17)
N5–Sn3	2.456(5)	S5–Sn4	2.4039(16)
N7–Sn4	2.399(5)	S5–Ag4	2.4445(17)
N9–Sn5	2.388(6)	S5–Ag3	2.5345(18)
N11–Sn6	2.419(6)	S6–Sn4	2.4153(16)
N13–Sn7	2.362(5)	S6–Sn3	2.4173(16)
N15–Sn8	2.371(5)	S7–Sn5	2.3984(16)
N17–Sn9	2.423(5)	S7–Sn10	2.5073(16)

S8–Ag5	2.3666(16)	S19–Ag1	2.4003(15)
S8–Sn2	2.3981(16)	S19–Ag6	2.5453(16)
S8–Ag2	2.6702(18)	S19–Ag9	2.7071(16)
S8–Ag4	2.9040(16)	S20–Ag5	2.3823(16)
S9–Ag7	2.3851(16)	S20–Sn10	2.3960(16)
S9–Sn3	2.3923(15)	S20–Ag9	2.4738(16)
S9–Ag2	2.5411(16)	Ag1 ^{···} Ag2	2.9353(7)
S9–Ag4	2.7883(16)	Ag1 ^{···} Ag6	3.0539(7)
S10–Ag10	2.3856(16)	Ag2 ^{···} Ag3	2.9690(8)
S10–Sn5	2.3919(16)	Ag2 ^{···} Ag7	3.0108(7)
S10–Ag4	2.4641(17)	Ag3 ^{···} Ag4	3.1363(8)
S11–Sn6	2.4332(17)	Ag5 ^{···} Ag10	2.9640(7)
S11–Ag8	2.4847(17)	Ag6 ^{···} Ag7	2.9521(7)
S11–Sn7	2.5987(17)	Ag6 ^{···} Ag8	2.9847(8)
S12–Sn6	2.3909(16)	Ag6 ^{···} Ag9	3.3260(7)
S12–Ag7	2.4101(16)	Ag8 ^{···} Ag9	3.1388(7)
S12–Ag6	2.5075(17)	C1–Sn1–N1	71.6(2)
S13–Sn7	2.3925(16)	N1–Sn1–S3	171.01(15)
S13–Sn6	2.5513(16)	C7–Sn2–N3	74.7(2)
S14–Sn8	2.5174(16)	N3–Sn2–S1	169.03(12)
S14–Sn9	2.5221(16)	C13–Sn3–N5	73.7(2)
S14–Ag8	2.6364(18)	N5–Sn3–S4	166.07(12)
S15–Sn9	2.3865(17)	C19–Sn4–N7	74.2(2)
S15–Ag9	2.4504(17)	N7–Sn4–S4	175.63(13)
S15–Ag8	2.5633(18)	C25–Sn5–N9	75.7(3)
S16–Sn9	2.4248(16)	N9–Sn5–S17	176.72(15)
S16–Sn8	2.4503(15)	C31–Sn6–N11	75.1(2)
S17–Sn10	2.3967(15)	N11–Sn6–S13	171.24(14)
S17–Sn5	2.5352(16)	C37–Sn7–N13	75.8(2)
S18–Ag10	2.3686(16)	N13–Sn7–S11	168.09(13)
S18–Sn7	2.4000(16)	C43–Sn8–N15	75.7(2)
S18–Ag6	2.6424(18)	N15–Sn8–S14	171.53(13)
S18–Ag9	2.8639(16)	C49–Sn9–N17	74.8(2)
S19–Sn8	2.3992(15)	N17–Sn9–S14	172.70(14)

C55–Sn10–N19	74.1(2)	S8–Ag5–S20	169.97(6)
N19–Sn10–S7	179.10(14)	S12–Ag6–S19	141.77(5)
S19–Ag1–S2	167.86(6)	S9–Ag7–S12	169.56(6)
S2–Ag2–S9	144.28(6)	S11–Ag8–S15	141.15(6)
S1–Ag3–S5	133.81(6)	S15–Ag9–S20	138.05(6)
S5–Ag4–S10	143.31(6)	S18–Ag10–S10	166.77(6)

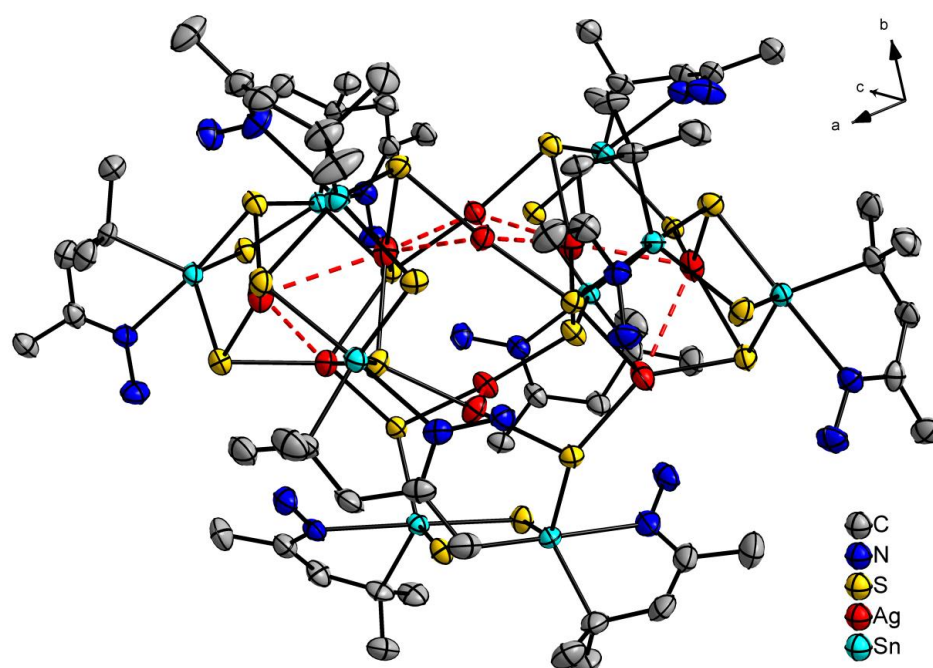


Figure S6. Molecular structure of **4** without disorder. H atoms are omitted for clarity.
Thermal ellipsoids are drawn at 50% probability.

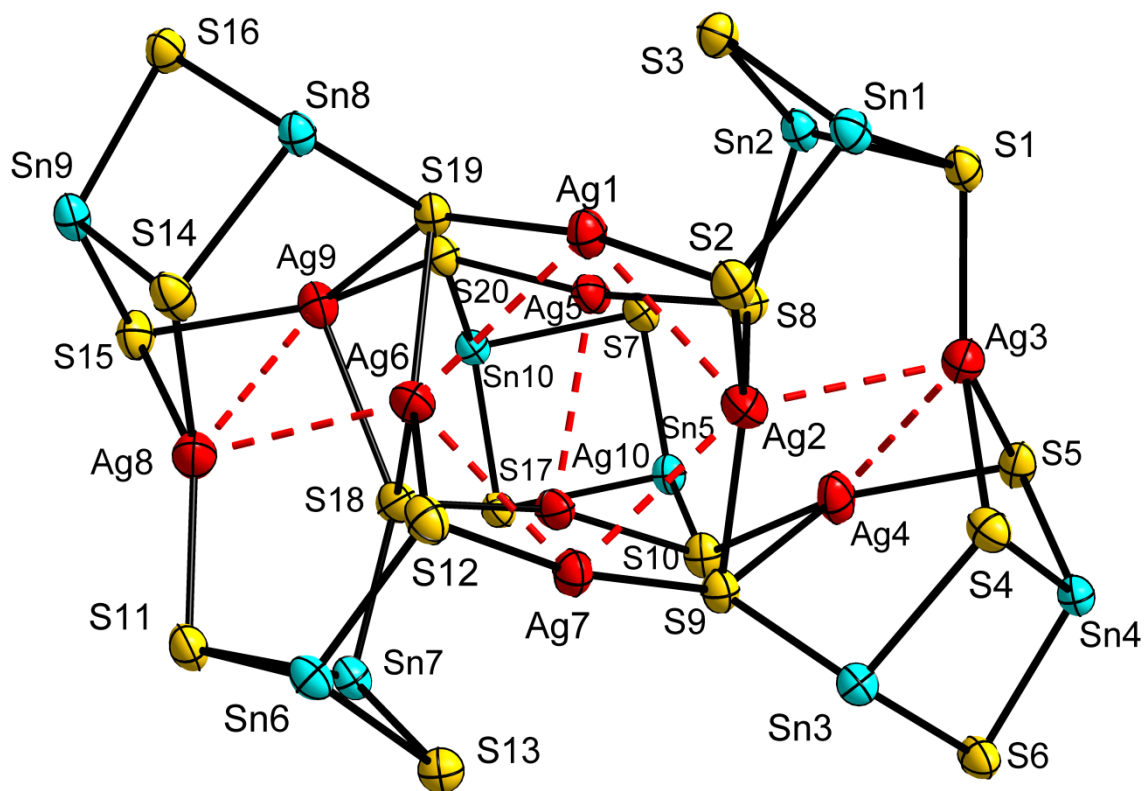


Figure S7. Molecular structure of the inorganic core of **4** with atom labeling scheme for. View along the pseudo C_2 -axis. Thermal ellipsoids are drawn at 50% probability.

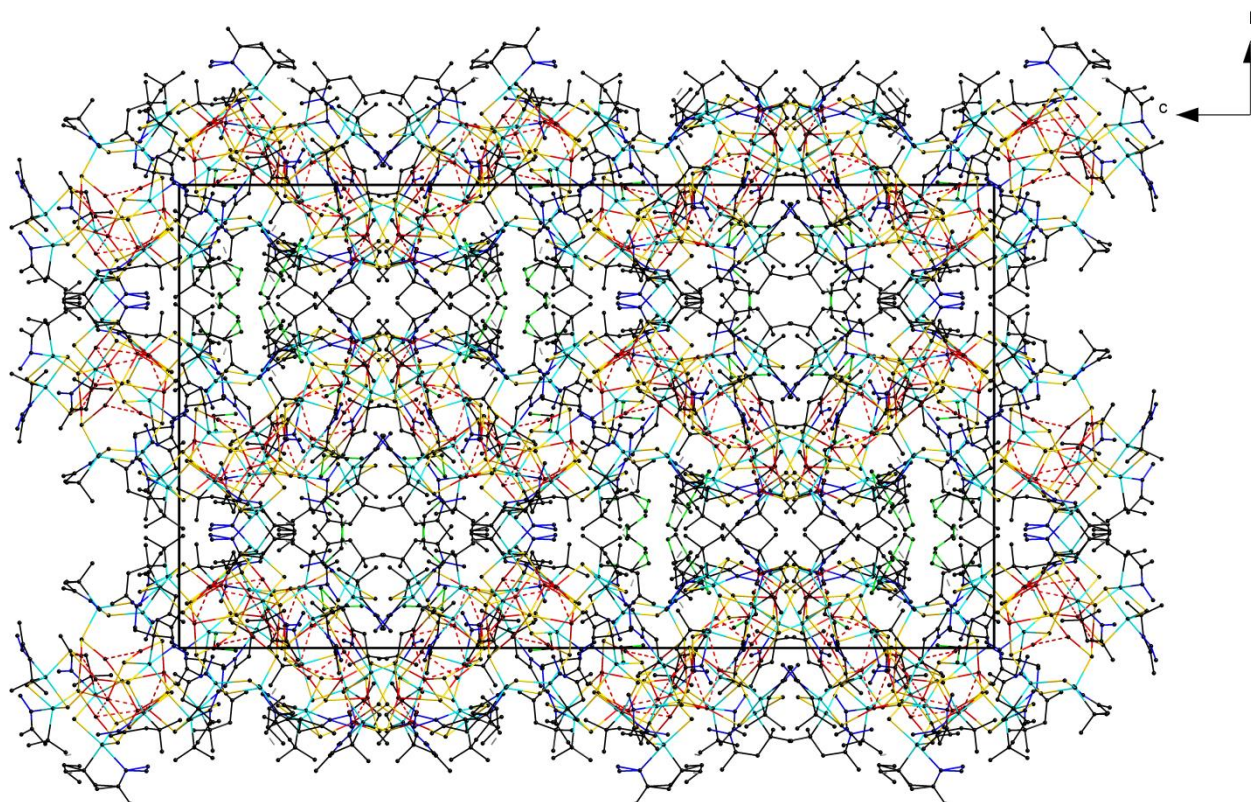


Figure S8. View along $[100]$ in $4 \cdot 3.5\text{CH}_2\text{Cl}_2$. H atoms are omitted for clarity.

Compound 5: The compound crystallizes in the monoclinic space group $P2_1/c$ with $Z = 2$. The highest peak of $1.97 \text{ e}/\text{\AA}^3$ on the difference Fourier map was observed 1.02 \AA apart from Au1. Selected intermolecular parameters are outlined in Table S5.

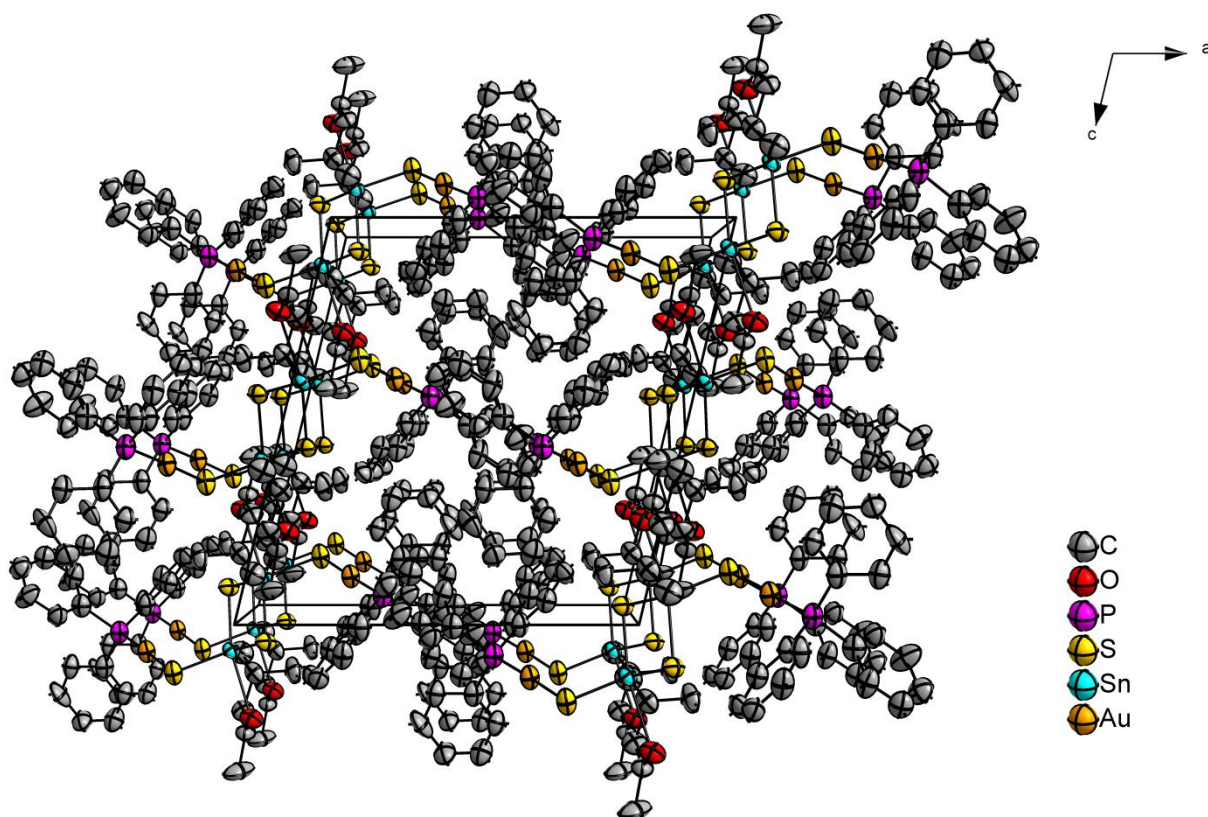


Figure S9. View along $[010]$ in **5**. H atoms are omitted for clarity. Thermal ellipsoids are drawn at 50% probability.

Compound 6: The compound crystallizes with 5 molecules of dichloromethane per formula unit in the triclinic space group $P\bar{1}$ with $Z = 1$. The quality of the measurement was limited due to very thin plates of **6** that decomposed rapidly in inert oil likely because of loss of solvent molecules. H atoms from hydrazone moieties were on the difference Fourier map and refined with DFIX restraint of 0.88 Å for the N–H-bond length and $n = 1.5$. The highest peak of $2.85 \text{ e}/\text{Å}^3$ on the difference Fourier map was observed 1.03 Å apart from Au1. Selected intermolecular parameters are outlined in Table S5.

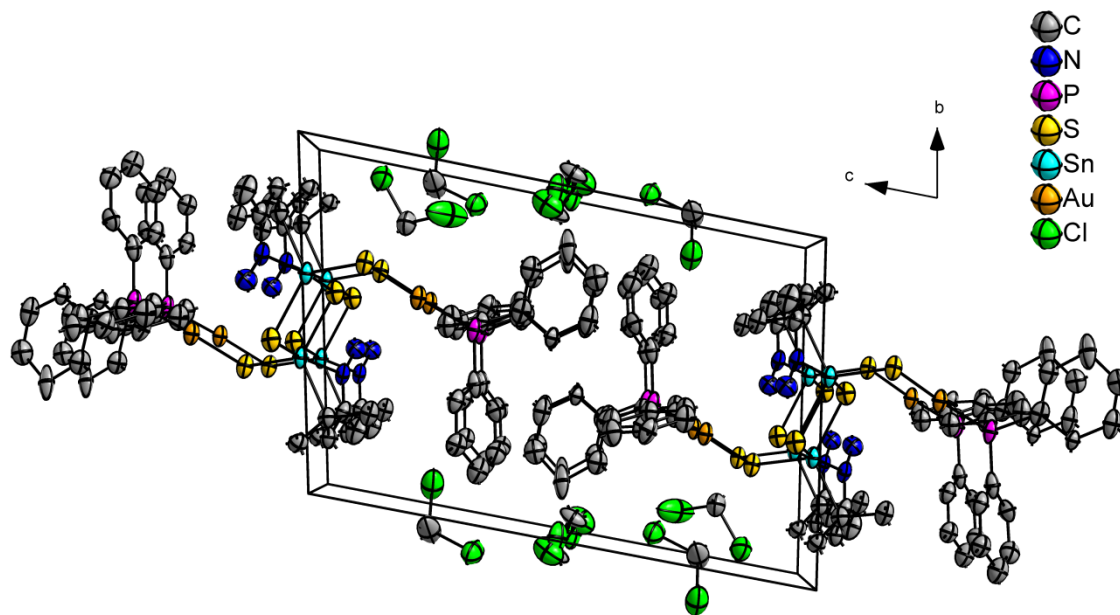


Figure S10. View along [100] in **6**·5CH₂Cl₂ without disorder. H atoms are omitted for clarity. Thermal ellipsoids are drawn at 50% probability.

Table S5. Selected structural parameters [\AA , $^\circ$] of **5** and **6** \cdot 5CH₂Cl₂ (X = O1 (**5**) or N1(**6**)).

compound	5	6 \cdot 5CH ₂ Cl ₂
Sn1–C1	2.189(8)	2.186(14)
Sn1–X1	2.714(6)	2.479(11)
Sn1–S1	2.402(2)	2.421(4)
Sn1–S1 ^{b,c}	2.463(2)	2.525(3)
Sn1–S2	2.380(2)	2.389(3)
Au1–S2	2.291(2)	2.298(3)
Au1–P1	2.260(2)	2.250(3)
X1–Sn1–S1 ^{b,c}	165.38(2)	167.4(3)
X1–Sn1–C1	68.9(3)	72.8(4)
S1–Sn1–S1 ^{b,c}	93.70(7)	90.94(11)
S1–Sn1–S2	110.22(9)	116.10(13)
S1 ^{b,c} –Sn1–S2	110.70(9)	107.39(11)
S1–Au1–P1	178.29(9)	172.84(12)
Sn1–S1–Sn1 ^{b,c}	86.30(7)	89.06(11)
Sn1–S2–Au1	96.63(9)	103.86(13)

symmetry code: b = $-x, 2-y, 1-z$ (**5**), c = $2-x, 1-y, -z$ (**6**).

(Me₃Si)₂S: The compound crystallizes in the monoclinic space group *C2/c* with *Z* = 4. The X-ray measurement was of limited quality. Even very slow cooling-down the compound in a glass capillary hardly gave crystals suitable for diffraction experiments. The obtained dataset was twinned and therefore a hklf5-file was used for refinement (BASF = 0.383(6)). The dataset was merged. The highest peak of 0.87 e/Å³ on the difference Fourier map was observed 1.01 Å apart from S1.

Selected structural parameters: Si1–S1 = 2.152(2) Å, Si1–C1 = 1.876(7) Å, Si1–C2 = 1.856(6) Å, Si1–C3 = 1.864(7) Å, Si1⋯Si1ⁱ = 3.493(3) Å, C1⋯C2ⁱ = 3.683(10) Å, Si1–E1–Si1ⁱ = 108.53(13)°; *i* = 1–*x*, *y*, 0.5–*z*.

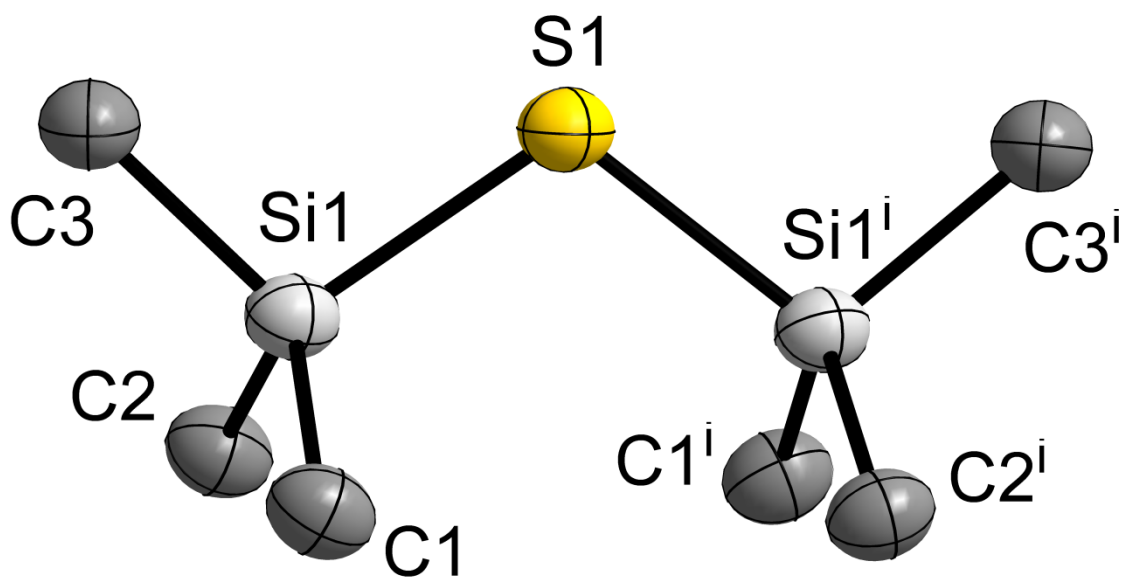


Figure S11. Molecular structure of (Me₃Si)₂S. H atoms are omitted.

Thermal ellipsoids are drawn at 30% probability.

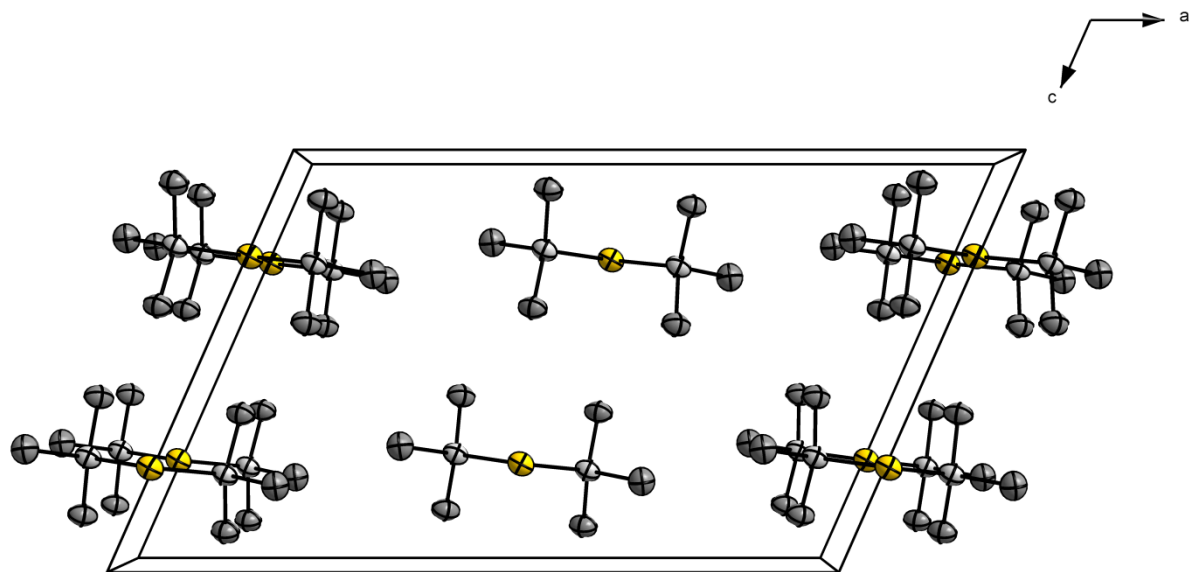


Figure S12. View along $[010]$ in $(\text{Me}_3\text{Si})_2\text{S}$. H atoms are omitted for clarity. Thermal ellipsoids are drawn at 30% probability.

3. Density functional theory (DFT) calculations

Methods of the quantum chemical investigation: For DFT calculations the program system TURBOMOLE Version 6.2⁶ using the RIDFT⁷ program with the BP86 functional⁸ and gridsize m3 was used. Basis sets were of def2-TZVP quality.^{9,10} For Sn atoms effective core potentials (ECP-28)¹¹ have been used. No symmetry restrictions (*i.e.* C_1 symmetry) during simultaneous optimizations of geometry and electronic structure were hold. The accuracy of the structures was found within the typical error of the method. Natural Population Analysis was performed within the program system after the reported method.¹² The results of the analysis are provided in Table S6 for selected atoms.

Table S6. Results of the charges for selected atoms, as calculated by Natural Population Analysis of $[(R^I Sn)_4(SnCl)_2(CuPPh_3)_2S_8]$ and $[(R^I Sn)_4(SnCl)_2(AgPPh_3)_2S_8]$.

	formal oxidation state	$[(R^I Sn)_4(SnCl)_2(CuPPh_3)_2S_8]$	$[(R^I Sn)_4(SnCl)_2(AgPPh_3)_2S_8]$
$(R^I)Sn$	+IV	+1.38/+1.47	+1.37/+1.44
$(Cl)Sn$	+II	+0.88	+0.81
Cu/Ag	+I	+0.66	+0.62
P	(formal charge: +1)	+0.79	+0.80
Cl	-I	-0.60	-0.59

References for the supporting information

- 1 J. P. Eußner, B. E. Barth, E. Leusmann, Z. You, N. Rinn and S. Dehnen, *Chem. Eur. J.*, 2013, **19**, 13792-13802.
- 2 J.-H. So and P. Boudjouk, *Synthesis*, 1989, 306-307.
- 3 P. Strauch and L. Golic, *Z. Anorg. Allg. Chem.*, 1996, **622**, 1236-1240.
- 4 A. Cassel, *Acta Crystallogr.*, 1981, **B37**, 229-231.
- 5 G. M. Sheldrick, *Acta Crystallogr.*, 2008, **A64**, 112-122.
- 6 TURBOMOLE V.6.2, © TURBOMOLE GmbH 2011. TURBOMOLE is a development of University of Karlsruhe and Forschungszentrum Karlsruhe 1989-2007.
- 7 (a) K. Eichkorn, O. Treutler, H. Öhm, M. Häser and R. Ahlrichs, *Chem. Phys. Lett.*, 1995, **242**, 652–660; (b) K. Eichkorn, F. Weigend, O. Treutler and R. Ahlrichs, *Theor. Chim. Acta*, 1997, **97**, 119–124.
- 8 (a) A. D. Becke, *Phys. Rev. A*, 1988, **38**, 3098-3100; (b) S. H. Vosko, L. Wilk and M. Nusair, *Can. J. Phys.*, 1980, **58**, 1200-1205; (c) J. P. Perdew, *Phys. Rev. B*, 1996, **33**, 8822-8824.
- 9 F. Weigend and R. Ahlrichs, *Phys. Chem. Chem. Phys.*, 2005, **7**, 3297-3305.
- 10 F. Weigend, *Phys. Chem. Chem. Phys.*, 2006, **8**, 1057–1065.
- 11 B. Metz, H. Stoll and M. Dolg, *J. Chem. Phys.*, 2000, **113**, 2563-2569.
- 12 A. E. Reed, R. B. Weinstock and F. Weinhold, *J. Phys. Chem.*, 1985, **83**, 735-746.